

# Mould growth assessment of internally insulated advanced envelopes: A parametric study and the notion of the multi-variable design-assessment charts

Mohamad Ibrahim<sup>1</sup>, Marina Stipetic<sup>2</sup>, Etienne Wurtz<sup>1</sup>, Jürgen Frick<sup>2</sup>

<sup>1</sup>Univ. Grenoble Alpes, CEA, LITEN, INES, F-38000 Grenoble, France

<sup>2</sup>Materials Testing Institute, University of Stuttgart, Otto-Graf-Institute, D-70569 Stuttgart, Germany

## Abstract

In this study, we investigate the impact of retrofitting intervention through adding super-insulation panels based on subcritical-dried (ambient pressure dried) aerogels as interior insulation on the hygrothermal performance of brick walls. The aim is to compare the hygrothermal performance of different wall configurations and to examine the effect of various design or climatic parameters. Simulations are carried out using WUFI and the mould growth index according to the *VTT* model is considered as the assessment parameter. Results are sensitive to the specific simulation cases. For this reason, a simulation-based multi-variable design assessment chart for mould growth risk is here proposed.

## Introduction

The 2012/27/UE Directive has established a common framework for the promotion of the energy efficiency in Europe and has underlined the importance of the renovation of the existing building stocks because they represent the biggest potential sector for energy savings. The share of the building sector is about 43% of the total energy consumption and 25% of carbon dioxide emission. Super-insulating materials, such as silica aerogels, are promising materials for the building sector to obtain the desired objectives. Other than energy efficiency, the moisture performance is a key consideration in the building envelope design.

The hygrothermal performance of existing exterior walls will be highly influenced when adding interior thermal insulation, especially if advanced materials are used. The hygrothermal properties of the added insulation material, such as vapour openness and capillarity, influence the performance of the whole wall structure. In the cold climates, insulating the exterior walls on the interior side reduces the drying potential due to the reduced heat flows coming from the interior heated space. In this case, mould can appear when favorable conditions are present. In general, the risk of failure will be higher if thicker interior insulation is used (Alev and Kalamees 2016) and, consequently, may induce a risk on interstitial condensation, frost damage, mould growth and other damage patterns.

Several studies have dealt with the subject of the exterior walls' retrofitting and the hygric risks associated with the installation of interior thermal insulation. Johansson et al. (2014) investigated the hygrothermal performance of a

brick wall with wooden beam ends after the wall was insulated on the interior side with vacuum insulation panels (VIP). There was no significant difference between the relative humidity in the wooden beam ends for the cases with and without the VIPs. However, they found that the reduced temperature in the brick after the VIPs were added led to a higher relative humidity in the wooden beams. Moreover, when VIPs were added on the interior side, the drying capacity to that side of the wall was substantially reduced.

Harrestrup and Svendsen (2016) studied the use of internal insulation in a heritage building block with wooden beam construction and masonry brick walls regarding energy renovation. The risk of mould growth in the wooden beams and in the interface between the insulation and the brick wall was evaluated for various internal insulation. According to this study, it is not recommended to apply internal insulation on north-orientated walls, since the drying potential is reduced.

Vereecken and Roels (2014) examined the hygric performance of walls with different interior insulation systems exposed to a quasi-steady-state winter condition based on a hot box–cold box experiment. They showed that a vapour tight system is preferable to a capillary active interior insulation system from the point of view of interstitial condensation.

Toman et al. (2009) carried out an in-situ assessment of hygric and thermal performance of an interior thermal insulation system based on hydrophilic mineral wool and without water vapour barrier. The insulation system is applied on an old brick house. According to the authors, the wall construction showed a good moisture behavior.

In this study, we investigate the impact of the retrofitting intervention through adding super-insulation panels based on subcritical-dried (ambient pressure dried) aerogels as interior insulation on the hygrothermal performance of the exterior walls. The performance of the wall covered with different exterior plasters/renders is examined. The aim is to compare the hygrothermal performance of the different wall configurations and to examine the effect of various parameters on this performance.

## Wall construction materials

The performance of brick walls subjected to the retrofit solution by adding the aerogel-based insulation at the interior surface is considered in this study (see Figure 1).

Table 1: The hygro-thermo-physical properties of the construction materials

(a)

Material	Density [kg/m <sup>3</sup> ]	Porosity [%]	Specific heat (dry) [J/(kg.K)]	Thermal conductivity (dry, 10°C) [W/(m.K)]	Water vapour diffusion resistance factor $\mu$ [-]
Solid brick	1900	24	850	0.6	10
Historical brick	1800	31	850	0.6	15
Aerogel panel	110	0.90	1000*	0.0148	6.1 (wet-cup-method) 4.2 (dry-cup-method)
Exp. Polystyrene	15	95	1500	0.04	30
Mineral wool	60	95	850	0.04	1.3
Calcium silicate	270	0.9	1162	0.063	3.8
Interior plaster (gypsum)	850	65	850	0.2	8.3

(b)

Exterior plaster	Density [kg/m <sup>3</sup> ]	Porosity [-]	Specific heat (dry) [J/(kg.K)]	Thermal conductivity (dry, 10°C) [W/(m.K)]	Water vapour diffusion resistance [-]	Water absorption coefficient [kg/(m <sup>2</sup> h <sup>0.5</sup> )]
P.1 (mineral)	1900	0.24	850	0.8	25	0.1
P.2 (cement)	2000	0.3	850	1.2	25	0.51
P.3 (cement lime 1)	1900	0.24	850	0.8	19	1
P.4 (cement lime 2)	1266	0.52	359	0.354	12	1.5
P.5 (cement lime 3)	1900	0.24	850	0.8	19	2
P.6 (lime 1)	1600	0.3	850	0.7	7	3
P.7 (lime 2)	1432	0.46	630	0.3034	11	4.8
P.8 (Hydraulic lime)	1830	0.27	850	0.7	19.99	6.12
P.9 (lime cement)	1024	0.61	850	0.179	3.1	7.6
P.10 (lime 3)	1600	0.33	850	0.7	12	10.2

\* Not measured; estimated from literature data

All materials are selected from the IBP-WUFI (IBP WUFI® Pro v 5.3) database, except the aerogel panel whose properties are measured at lab-scale and presented in the following section. The main characteristics of the materials used in this study are shown in Table 1.

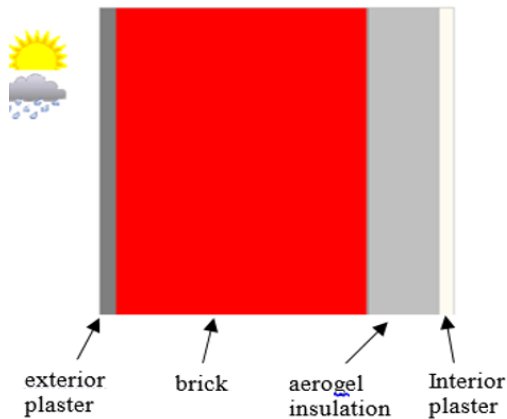


Figure 1 : The retrofitting solution by adding the aerogel-based panel as interior insulation system

We selected Ten exterior plasters according to their water vapour diffusion resistance factor ( $\mu$ ) and water absorption coefficient ( $A_{cap}$ ). The water vapour diffusion resistance affects the moisture transport in the vapour

state and the water absorption coefficient affects the moisture transport in the liquid state. According to standard EN 998-1 (2010), the mineral renders and plasters are classified in three classes according to their  $A_{cap}$  value as shown in Table 2. The  $A_{cap}$  value indicates the speed by which the moisture front propagates when the material is in direct contact with liquid water. The selected plasters cover a wide range of possible materials that can be applied on the exterior surface of the building envelope. Hereby, various combinations of capillary absorption coefficients and vapour diffusion resistance values are used.

The first four plasters lie in the W2 class with  $A_{cap}$  less than 1.56 kg/(m<sup>2</sup>h<sup>0.5</sup>). P.1 and P.2 have the same, relatively high  $\mu$  value ( $\mu = 25$ ) but different  $A_{cap}$  values. P.1 has the lowest  $A_{cap}$ , [0.1 kg/(m<sup>2</sup>h<sup>0.5</sup>)], meaning that it has a very low capillary uptake capacity, while P.2 has a higher value [ $A_{cap} = 0.51$  kg/(m<sup>2</sup>h<sup>0.5</sup>)]. P.3 has a higher  $A_{cap}$  than the last two plasters associated with a lower vapour diffusion resistance value ( $\mu = 19$ ). P.4 has a higher  $A_{cap}$  and a lower  $\mu$  value than P.3.

P.5 has the same  $\mu$  value as that of the plaster P.3; however, it has a higher  $A_{cap}$ , making it a W1-class plaster. P.6 is also in the W1-class zone but it has a low vapour diffusion resistance ( $\mu = 7$ ).

The last four plasters (P.7, P.8, P.9 and P.10) lie in the W0 class with  $A_{cap}$  more than  $3.11 \text{ kg}/(\text{m}^2\text{h}^{0.5})$ . In comparison to other used plasters, P.9 has the lowest  $\mu$  value and P.10 has the highest capillary absorption value; i.e. the plaster that absorbs the highest amount of liquid water in the shortest time, when it is in contact with a liquid source.

To illustrate the hygric properties of the different exterior plasters used in this study, the combination of the water absorption coefficient ( $A_{cap}$ ) and the water vapour diffusion resistance ( $\mu$ ) of each of these plasters is shown in Figure 2.

Table 2: Exterior plaster classes

Class	Water absorption coefficient
W0	No limit
W1	$A_{cap} < 0.4 \text{ kg}/(\text{m}^2\text{min}^{0.5})$ [ $3.11 \text{ kg}/(\text{m}^2\text{h}^{0.5})$ ]
W2	$A_{cap} < 0.2 \text{ kg}/(\text{m}^2\text{min}^{0.5})$ [ $1.56 \text{ kg}/(\text{m}^2\text{h}^{0.5})$ ]

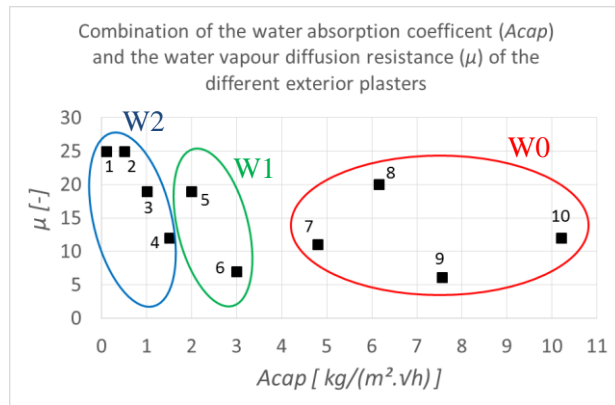


Figure 2 : Combination of the water absorption coefficient ( $A_{cap}$ ) and the water vapour diffusion resistance ( $\mu$ ) of the different exterior plasters

## The ambient-dried aerogel-based insulating panels

Nowadays, there is a high interest and research on super-insulating materials for building applications, particularly aerogels (Galliano et al. 2016, Ibrahim et al. 2015, Mujeebu et al. 2016).

In this context, new ambient-dried silica advanced aerogel-based composite insulating materials reinforced by glass fibers are developed. The newly developed material can be applied for new buildings as well as for old buildings. It can be used as internal and external insulation. The hygrothermal and physical properties of the newly developed aerogel-based insulating panel are measured at lab scale at the Materials Testing Institute, University of Stuttgart.

In comparison to other aerogel-based insulation available on the market, the developed insulation in scope of this work has an improved manufacturing process in order to reduce the production costs of aerogels. Moreover, the

panels are available in various thicknesses, from 0.5cm up to 3cm.

The influence of moisture content was tested for moisture absorption and desorption (Table 3). Samples were preconditioned at  $23^\circ\text{C}$  and 50% relative humidity or dried at  $70^\circ\text{C}$  prior to testing. Dry specimens were stored at the target relative humidity from 50 or 80% until steady state (no further change in specimen weight). On the other hand, preconditioned specimens ( $23^\circ\text{C}$  and 50% relative humidity) were dried. The change of mass was estimated. Measurement of thermal conductivity was performed for all three conditioning levels, namely  $23^\circ\text{C} / 50\% \text{ RH}$ ,  $70^\circ\text{C}/0\% \text{ RH}$  (dry) and  $23^\circ\text{C}/80\% \text{ RH}$ . Thermal conductivity was measured acc. to EN 12667 standard. Results in Table 3 show negligible influence of humidity on the thermal conductivity of the aerogel-based insulating panels.

Table 3 : Influence of humidity on the thermal conductivity of the aerogel-based insulating panels

Conditioning	Diff. of mass $\Delta m$ [%]	Thermal conductivity $\lambda$ [ $\text{W}/(\text{m}\cdot\text{K})$ ]
<b><math>23^\circ\text{C}</math>, 50% RH</b>	+1.0	0.01499
<b><math>70^\circ\text{C}</math>, 0% RH (dry)</b>	-1.1	0.01487
<b><math>23^\circ\text{C}</math>, 80% RH</b>	+2.6	0.01506

Water vapour permeability was determined according to EN 12086 and EN ISO 12572 standards. Samples were preconditioned at  $23^\circ\text{C}$  and 50% relative humidity prior to testing. Hereby, “dry-cup-method”, for the humidity range from 0 to 50% RH, and “wet-cup-method”, for the range from 50 to about 100% RH are performed. The developed aerogel-based insulating panel (Table 1) shows expected behaviour to water vapour permeability relating to reference values of mineral wool ( $\mu = 1$ ), wood fiber insulation ( $\mu = 1-3$ ), as well as the performance of polystyrene, extruded polystyrene and polyurethane foam ( $\mu = 60-150$ ).

Water absorption was tested acc. to EN 1609 (short-term water absorption) and EN 12087 (long-term water absorption) for partial immersion of specimen in water. Specimens were conditioned at  $23^\circ\text{C}$  and 50% relative humidity before test. Test results are presented in Table 4. These are compared to provisions given by EN 13162 for mineral wool.

Table 4 : Water absorption tests

Test	Water absorption [ $\text{kg}/\text{m}^2$ ]	Requirements acc. to EN 13162 [ $\text{kg}/\text{m}^2$ ]
Short term (24h) water absorption	0.12	$\leq 1$
Long term (28d) water absorption	0.41	$\leq 3$

## Assessment criterion

Different mould growth prediction models are found in the literature. Some are simple qualitative models (Time of wetness, *RHT* index, ASHRAE standard-160 method) and others are more quantitative models (*VTT* model). Each of these models includes however different simplifications or is based on different assumptions. Vereecken and Roels (2012) have done an extensive review of the mould growth prediction models found in the literature presenting the drawbacks of each of these models based on the simplified assumptions used or the methodology followed. They have concluded that furthermore, more in-depth study of the mould growth, especially, under transient conditions is still necessary through undertaking additional measurements in lab conditions as well as in real ones.

In this study, we choose the *VTT* model to assess the envelope moisture performance because it is a dynamic model that takes into account the influence of temperature, relative humidity, surface, exposure time and dry periods.

### The *VTT* mould growth model

The *VTT* model is a dynamic model which was developed by Viitanen (1996) at the VTT Technical Research Center of Finland. It is an empirical mould prediction model in which the growth development is expressed by the mould index (*M*). This index ranges between 0 and 6 (Table 5) and can be used as a design criterion, for e.g. a mould index equals to 1 is often defined as the maximum tolerable value since from that moment the germination process is assumed to start.

Table 5 : Mould growth index classification (Viitanen et al. 2011)

Mould Index ( <i>M</i> )	Growth rate	Description
0	No mould growth	Spores not activated
1	Small amounts of mould on surface	Initial stages of growth
2	<10% coverage of mould on surface	New spores produced
3	10-30% coverage of mould on surface	
4	30-70% coverage of mould on surface	Moderate growth
5	>70% coverage of mould on surface	Plenty growth
6	Dense mould growth covers nearly 100% of the surface	Coverage around 100%

The *VTT* model is based on regression analysis of a set of measured data. Based on the different measurements, the influence of temperature, relative humidity, surface, exposure time and dry periods is included in the *VTT* model.

The model was initially developed for pine and spruce sapwood materials based on lab experiments, and

afterwards it was expanded for other building materials (Ojanen et al. 2011). The models define the materials according to four mould sensitivity classes: very sensitive, sensitive, medium resistant and resistant. Table 6 gives the sensitivity classes together with the subdivision of the tested materials and an overview of the materials that belong to the different classes.

The *VTT* mathematical model is not presented here; however, it can be found in details in Viitanen et al. (2011).

Table 6: Materials' sensitivity classes (Viitanen et al. 2011)

Sensitivity class	Tested materials	Material group
<b>Very sensitive (vs)</b>	Pine sapwood	Untreated wood: includes lots of nutrients
<b>Sensitive (s)</b>	Glued wooden boards, Polyurethane with paper surface, spruce	Planed wood: paper-coated products, wood-based boards
<b>Medium resistant (mr)</b>	Concrete, aerated and cellular concrete, glass wool, polyester wool	Cement or plastic based materials, mineral fibers
<b>Resistant (r)</b>	Polyurethane with polished surface	Glass and metal products, materials with efficient protective compound treatments

## Modeling approach

### Numerical model

The software WUFI® Pro 5.3 is used to solve the transient coupled one-dimensional heat and moisture transport in a multi-layer building components. WUFI® was used in several studies to assess hygrothermal performance of building facades. Its accuracy has been tested through numerous field studies of different building components such as building facades, roofs and foundations.

WUFI® uses the temperature and the relative humidity as the driving potentials. The governing equations for heat and moisture transport are given in equations (1) and (2), respectively.

$$\frac{\partial H}{\partial T} \frac{\partial T}{\partial t} = \nabla (k \nabla T) + h_v \nabla (\delta_p \nabla (\varphi P_{\text{sat}})) \quad (1)$$

$$\frac{\partial w}{\partial \varphi} \frac{\partial \varphi}{\partial t} = \nabla (D_\varphi \nabla \varphi + \delta_p \nabla (\varphi P_{\text{sat}})) \quad (2)$$

where *H*, *T*, *w* and *φ* are the enthalpy, temperature, moisture content, and relative humidity, respectively. *P<sub>sat</sub>*, *k*, *h<sub>v</sub>*, *δ<sub>p</sub>* and *D<sub>φ</sub>* are the saturation pressure, thermal conductivity, evaporation enthalpy of water, water vapour permeability, and liquid conduction coefficient, respectively.

For the numerical solution, WUFI® uses the finite volume technique for the spatial discretization of the transport equations, the fully implicit scheme for the discretization in time.

## Boundary conditions

In this study, the climate of the city of Munich (Germany) is chosen as the outside boundary condition for the simulations. The weather file provided in WUFI was used. The German National Meteorological Service provides this weather file (TMY), which represents a test reference year representing typical weather situations. The weather test year is constructed based on 30-years mean values. The outside air temperature and relative humidity are shown in Figure 3. Using the climate analysis tool provided by WUFI®, the minimum outdoor temperature reaches  $-17.9^{\circ}\text{C}$  and the mean outdoor temperature is  $8.0^{\circ}\text{C}$  with a mean relative humidity of 78%. A north-west orientation of the wall is selected, as it is assessed to be most critical in terms of rain loads and lack of solar radiation.

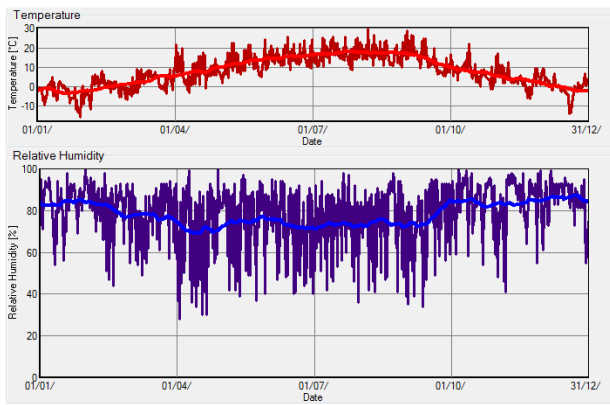


Figure 3: The outside air temperature and relative humidity for the climate of Munich

In WUFI® Pro, there are several methods to assign an indoor climate. In this study, the indoor conditions are determined in relation to the exterior climate according to the European standard DIN EN 15026 (2007) where, within certain limits, the indoor air temperature and the relative humidity depend linearly on the outdoor temperature, while outside of these limits they are kept constant as shown in Figure 4. In addition, two indoor moisture loads can be selected: a normal or a high moisture load.

## Simulation assumptions

As a base case, the indoor moisture load is considered as “Normal”. The outside solar absorptivity is taken as 0.5. The outside convective heat transfer coefficient is wind dependent. The exterior walls are considered to be in a building with a limited height (less than 10m). The latter has an effect on the rain exposure. The wall layers are assumed to have a perfect contact. Also, no air infiltration, e.g. due to cracks, is considered. Two wall structures built with solid masonry bricks and historical bricks are studied.

To calculate the *VTT* mould growth index ( $M$ ), the brick masonry is assumed to lie in the medium resistant class (refer to Table 6). The *VTT* model is written in MATLAB® to post-process the hygrothermal simulation

results of the WUFI® models. The  $M$  index is calculated at the critical position which is the interface between the brick and the aerogel insulation.

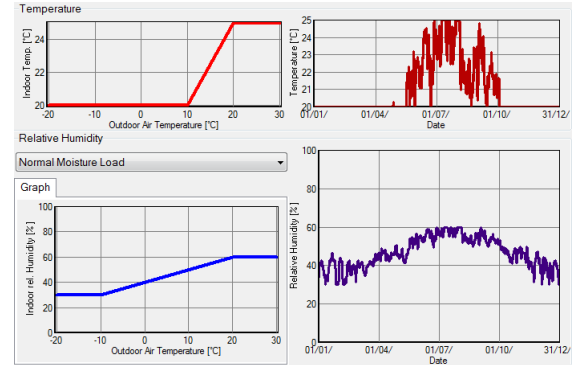


Figure 4: Indoor air temperature and relative humidity according to EN 15026 standard method

## Results

### Comparison of 10 exterior plasters

The mould growth index ( $M$ ) of the solid masonry brick wall insulated internally by 5cm thick aerogel panel is shown in Figure 5 for 10 different exterior plasters as well as for the un-plastered wall. Figure 5 shows that the walls with the exterior plasters P.1 and P.2 have the lowest mould growth index compared to the other walls. The same behavior is obtained for the total water content. The worst cases are the walls covered with exterior plasters P.5 and P.8.

The exterior plaster P.1, with the lowest capillary absorption [ $A_{cap} = 0.1 \text{ kg}/(\text{m}^2\text{h}^{0.5})$ ] and with, relatively, a high vapour diffusion resistance factor ( $\mu = 25$ ) shows the best performance among all other plasters. The plaster P.2 has the same  $\mu$  value as that of P.1 but higher  $A_{cap}$  value ( $0.51 \text{ kg}/(\text{m}^2\text{h}^{0.5})$ ). This plaster shows worse performance than P.1.

The plasters P.3 and P.5 have the same  $\mu$  value ( $\mu = 19$ ), but different capillarity coefficients.  $A_{cap}$  of P.3 is  $1 \text{ kg}/(\text{m}^2\text{h}^{0.5})$  and that of P.5 is  $2 \text{ kg}/(\text{m}^2\text{h}^{0.5})$ . The  $M$  index and the total water content (and the relative humidity) of the wall with P.5 is much higher than those of P.3 due to the increased  $A_{cap}$  value.

We can conclude that higher water absorption coefficient ( $A_{cap}$ ) increases the water content and relative humidity inside the wall structure. Due to increased amount of water (due to rain) penetrating in the wall

The plasters P.6, P.7, P.9, and P.10 have much higher  $A_{cap}$  than that of P.5; however, their performance is better than that of P.5 ( $M$  index is much lower than that for P.5). These four plasters have high  $A_{cap}$  value associated with a relatively low vapour resistance ( $\mu$  varies between 3 and 12) indicating a drying potential as soon as the boundary conditions become favorable.



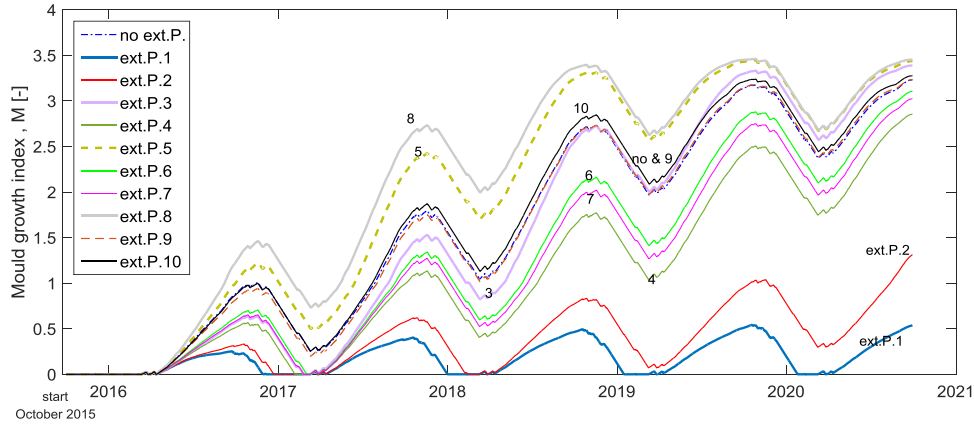


Figure 5 : The mould growth index ( $M$ ) for the brick masonry wall with different exterior plasters

The worst cases are P.8 and P.5. These plasters have higher capillarity transport along with high vapour diffusion resistance factor.

The simulation period is extended to 10 years to investigate the behavior of the wall construction with P.1 and P.2. The  $M$  index remains in the quasi-steady-state behavior as shown in Figure 6 for P.1; however,  $M$  increases significantly for P.2 and reaches values more than 3 indicating a high risk for mould growth (figure not shown for brevity).

From this analysis, we can conclude the following:

- It is the combination of the capillarity transport ( $A_{cap}$ ) and the vapour diffusion resistance factor ( $\mu$ ) that defines the performance of the exterior plaster
- The best plasters are those with very low capillarity transport (to prevent rainwater from getting in)
- There is a critical  $A_{cap}$ , where a plaster with a lower value than  $A_{cap}$  shows a good performance even if it has a high vapour diffusion resistance factor ( $\mu$ )
- For values higher than the critical  $A_{cap}$ , a plaster with a lower  $A_{cap}$  but with a high  $\mu$  will perform worse than a plaster with a higher  $A_{cap}$  and lower  $\mu$
- The worst case is the plaster having both a high  $A_{cap}$  and a high  $\mu$  (meaning water gets in and is difficult to get out)
- So if the exterior plaster has a high capillarity transport, it is essential to couple this property with a low vapour diffusion resistance factor to allow the wall to dry out.

Plaster P.1 shows the best behavior in this analysis. For this reason, P.1 is chosen for further parametric study.

## Parametric study

### Influence of the interior moisture load

In all shown simulations, the interior moisture load was calculated using the method of the EN 15026 standard with normal moisture load. In this section, the indoor moisture load is set to the high load. The mould growth index at the critical position of both investigated wall constructions, solid masonry brick (MB) and historical

brick (HB), with the selected plaster and under the normal and the high indoor moisture loads is shown in Figure 6.

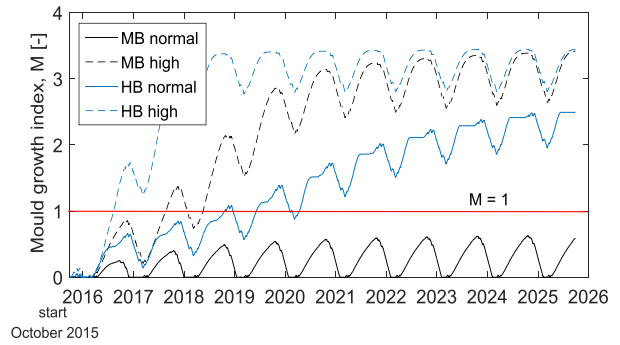


Figure 6 : The mould growth index ( $M$ ) at the critical position for solid masonry (MB) and historical brick (HB) wall construction insulated internally with 5cm of the aerogel panel under a normal and a high indoor moisture load

We extended the simulation period to ten years in order to show whether the behavior reaches a quasi-steady state. As illustrated in Figure 6, the increase in the interior moisture load has a drastic negative effect on the hygric performance of the wall assembly, especially for the solid masonry brick construction. For the latter, the risk of mould growth has increased significantly when the indoor moisture load is higher. The  $M$  index increases over 1 during the second year and its yearly average value continues to increase in a steep manner to reach a maximum value of around 3.4.

For the historical brick, the wall construction has high risk of mould growth even for the normal indoor moisture load. For this wall, the  $M$  index increases gradually when considering the normal load and increases rapidly to reach values more than 3 during the second year when considering the high load.

### Influence of the vapour barrier

A vapour barrier or retarder may be necessary to be installed behind the insulation layer near the interior wall surface especially when there is a high moisture flux coming from the interior space. Several vapour retarders with different vapour diffusion resistance factors or sd-values (sd-value is the vapour diffusion resistance factor " $\mu$ " multiplied by the material's thickness " $x$ ",  $sd = \mu \cdot x$ )

are tested for two wall assemblies (MB and HB). In case of the vapour retarder, the high moisture load for the indoor climate is chosen. The  $M$  index is shown in Figure 7 for the different sd-values of the vapour retarder.

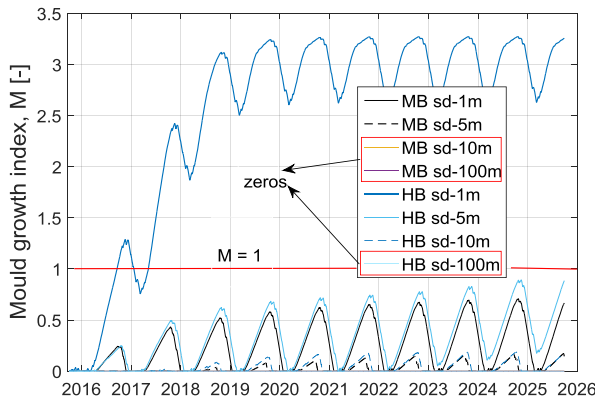


Figure 7 : The mould growth index ( $M$ ) at the critical position for solid masonry (MB) and historical brick (HB) wall construction insulated internally with 5cm of the aerogel panel under a high indoor moisture load for different vapour retarder sd-values

As illustrated in Figure 7, a vapour retarder with relatively high sd-value (high resistance to water vapour transmission) is needed to ensure a moisture safe wall construction, particularly for the historical brick wall construction with the 5cm thick aerogel panel.

For the historical brick wall with a vapour retarder having an sd-value of 1m, a significant mould growth risk is obtained starting from the second year of the simulation. For the HB wall with a vapour retarder having an sd-value of 5m, the yearly maximum " $M$ " index increases slightly over the years and shows a risk of mould growth after 12 years (for this case, simulation period to 15 years (figure not shown) to examine the curve behavior after 10 years and the risk to mould).

For the other vapour retarders (sd-10m and sd-100m), no risk of mould growth is observed. Thus, the selection of the vapour tightness of the vapour retarder is important in this case. For the solid masonry brick wall (MB) with the 5cm thick interior aerogel panel, all tested vapour retarders do not show any mould growth risks; however, the one that is more vapour tight behaves better than the one which is less vapour tight.

#### Influence of the rain exposure

Figure 8 shows the influence of the rain exposure to the mould growth index for the masonry brick and the historical brick walls. Two cases are considered: low building (height < 10m) and upper part of tall building (height > 20m). The latter one has much more rain absorption coefficient due to the higher rain exposure. Figure 8 shows that the higher rain exposure case does not show a significant difference from the lower rain exposure case for both the MB and the HB walls due to

the presence of the exterior render with very low capillarity.

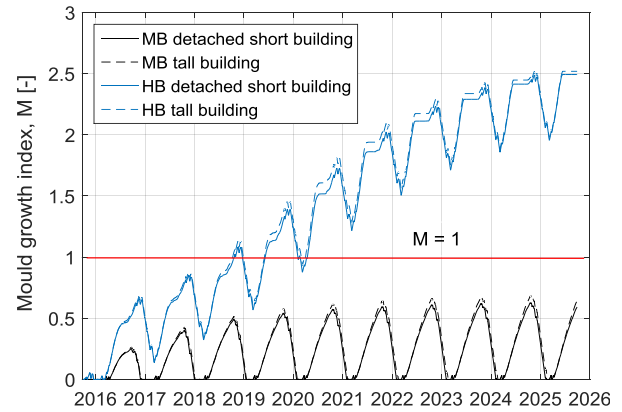


Figure 8 : The mould growth index ( $M$ ) at the critical position for solid masonry and historical brick wall construction insulated internally with 5cm of the aerogel panel for two rain exposure situations

#### Influence of rain penetration

In 2009, a comprehensive standard on moisture control design has been developed in North America (ANSI/ASHRAE Standard 160 2009). It proposes to consider rainwater leakage through the exterior cladding of exposed walls resulting from imperfections. The default value for water penetration through the exterior surface shall be 1% of the water reaching that exterior surface. A literature review (Van Den Bossche et al. 2011), analyzing data of leakage rates measured on different wall structures, confirmed the appropriateness of the '1% leakage' in ASHRAE Standard 160.

In this study, the rainwater leakage deposit position is considered to be the exterior layer of the load bearing masonry, so it is the position behind the exterior rendering. This can be considered as possible location due to cracks or poor workmanship. Simulations are carried out with the assumption of 1% rainwater leakage (with normal indoor moisture load and with normal rain exposure). As shown in Figure 9, initially the MB wall construction does not show a risk for mould growth; however, the risk starts to appear after the 11th year when considering the 1% rainwater leakage. For this case, the yearly maximum  $M$  index increases gradually throughout the years, and increases in a significant manner after the 11th year. For the HB wall construction (which has initially a high risk for mould growth even with no rainwater leakage), the rainwater leakage increases the  $M$  index additionally by about 0.5.

#### Comparison with traditional insulation materials

In this section, the moisture performance of the wall construction with the aerogel blanket is compared to the wall construction with mineral wool (MW) and expanded polystyrene (EPS), and also to the capillary active insulation material calcium silicate (CaSi).

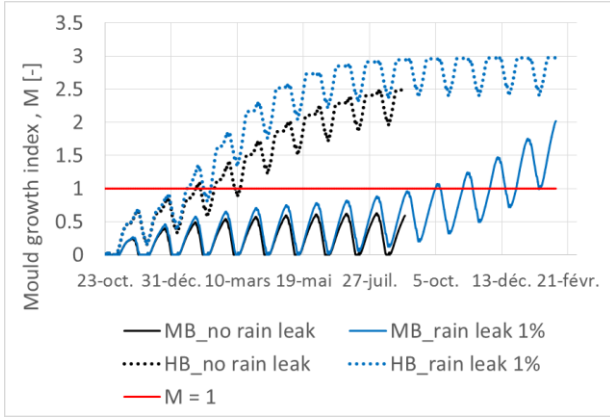


Figure 9 : The mould growth index ( $M$ ) at the critical position with the assumption of 1% rain water leakage behind the exterior render

For each of these insulation materials, two thicknesses are considered: the 5cm thickness as for the aerogel blanket and a thickness (14cm for MW and EPS and 22cm for CaSi) calculated in that manner to obtain the same thermal resistance ( $R$ -value) as for the aerogel blanket. The characteristics of these materials are previously shown in Table 1. For the comparison, the solid masonry brick is considered.

#### Case 1: No rain water leakage and normal indoor moisture load

Figure 10 shows the mould growth index at the critical position for the solid masonry wall construction with different thermal insulation materials and thicknesses (no rain water leakage and normal indoor moisture load). No risk of mould growth is observed for all cases. The performance of the “5cm thick aerogel panel” is close to that of the “14cm thick mineral wool”.

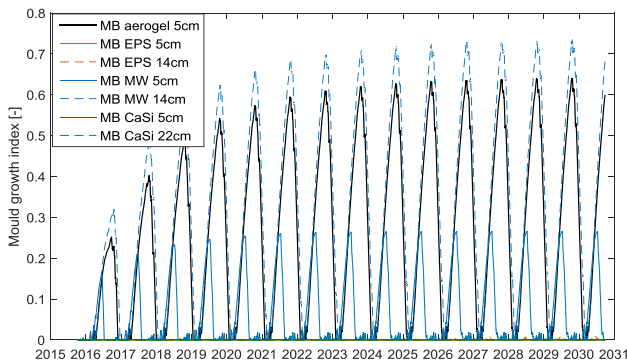


Figure 10: The mould growth index ( $M$ ) at the critical position for different internal thermal insulation for no rain water leakage and normal indoor moisture load

#### Case 2: No rain water leakage and high indoor moisture load

Figure 11 shows the mould growth index at the critical position for the solid masonry wall construction with the different thermal insulation materials and thicknesses for the case with no rain water leakage and high indoor moisture load.

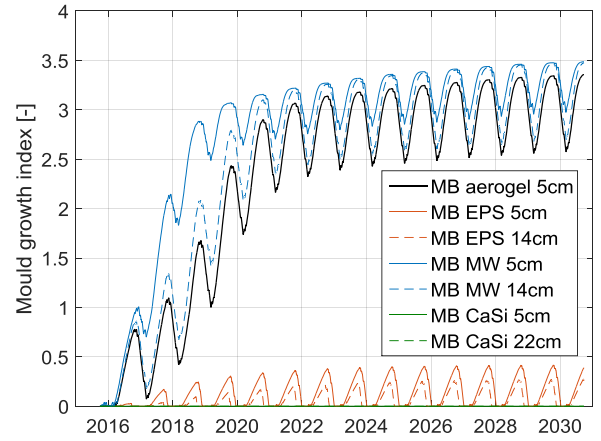


Figure 11: The mould growth index ( $M$ ) at the critical position for different internal thermal insulation for no rain water leakage and high indoor moisture load

It can be concluded from this figure that no potential for mould growth is observed for the insulating materials EPS and CaSi. EPS represents a vapour tight solution and CaSi a capillary active solution. EPS limits the vapour transfer from the inside to the outside while CaSi enhances the drying potential of the masonry layer to the inside due to the high capillarity characteristics. Both the aerogel panel and the mineral wool solutions which are vapour open materials fail in this case due to high indoor moisture load. Their vapour openness enhances the moisture transfer from the inside space.

#### Case 3: With rain water leakage and normal indoor moisture load

Figure 12 shows the mould growth index at the critical position for the case with rain water leakage and normal indoor moisture load. We can conclude that there is no potential for mould growth for the insulating materials EPS and CaSi.

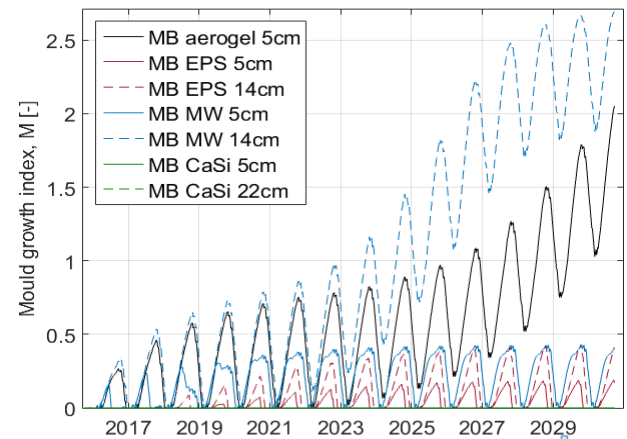


Figure 12: The mould growth index ( $M$ ) at the critical position for different internal thermal insulation with rain water leakage and normal indoor moisture load

On the contrary, MW which is a vapour open insulation material shows a significant and rapid risk for mould growth when applying the thickness of 14cm, and there is no risk when applying a thickness of 5cm. Even though the 14cm thick MW decreases the inside to outside vapour



transfer more than the 5cm thick MW, there is higher potential of drying out of the masonry structure to the inside (outside to inside flow) for 5cm MW (when the boundary conditions allow). This enhanced drying potential gives better behavior of the 5cm thick MW than for the 14cm thick MW.

For the aerogel blanket, there is a risk for mould growth which could be prevented by installing a vapour retarder at the inside surface of the insulation layer.

*Case 4: With rain penetration and high indoor moisture load*

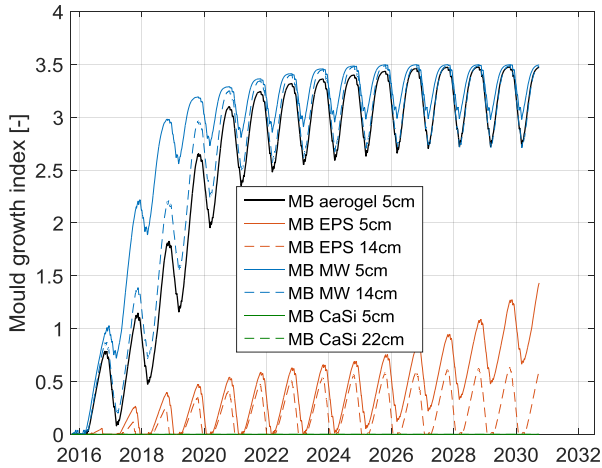


Figure 13 : The mould growth index ( $M$ ) at the critical position for different internal thermal insulation for rainwater leakage and high indoor moisture load

For the worst studied boundary conditions, rain leakage associated with a high indoor moisture load, the CaSi and the 14cm thick EPS constructions show moisture safe behavior as shown in Figure 13. All other constructions fail.

## Multi-parametric analysis and rapid design assessment chart

In the previous sections, we carried out a single variable parametric analysis to assess the hygric performance of the envelope with different construction techniques. However, it is shown that some variables, if coupled together, will have different effects on the envelope's hygric performance.

Accordingly, a multi-parametric analysis is needed where the mould growth index is estimated as a function of different parameters at the same time. For that reason, simulation-based multi-variable design-assessment chart is proposed that relates the  $M$  index to different variables. This kind of chart can serve as a rapid tool for designers to assess their construction performance at an early stage before carrying out detailed hygrothermal analysis.

Figure 14 shows the moisture design-assessment of the solid masonry brick wall construction insulated internally by the aerogel-based blanket. The assessment criterion is the mould growth index ( $M$ ). If  $M$  is greater than "1" during the simulation period taken as 15 years, the wall construction fails (F) the assessment criterion. If  $M$  is smaller than 1, it passes (P) the assessment criterion. The examined variables are: insulation thickness, indoor moisture load, rain exposure, rain water leakage, and vapour retarder sd-value.

Since the mould growth and humidity assessment is case sensitive and depends on several factors, the authors are currently working on developing a simple tool that accepts different design and climate parameters as inputs and generates an assessment chart similar to that shown in Figure 14, which can serve as an early-design assessment tool for building engineers.

Internal Insulation: aerogel blanket, Exterior Plaster 1 [ $A=0.1 \text{ kg}/(\text{m}^2 \cdot \text{Vh})$ , $\mu = 25$ ]									
climate: Munich, Orientation: NW, solid brick masonry (24cm)									
critical position: interface brick/insulation, simulation period: 15 years (start: october)									
assessment criterion: VTT mould growth index ( $M$ )									
		insulation thickness (cm)							
		2		3.5		5		7.5	
vapour retarder sd-value (m) (between insulation and inside plaster)	0	P	P	P	F	P	F	P	F
	1	P	P	P	P	P	P	P	P
	10	P	P	P	P	P	P	P	P
	100	P	P	P	P	P	P	P	P
	0	F	F	F	F	F	F	F	F
	1	P	F	P	F	P	F	P	F
	10	P	P	P	P	P	P	P	P
	100	P	P	P	P	P	P	P	P
	0	P	F	P	F	P	F	P	F
	1	P	F	P	F	P	F	P	F
	10	P	F	P	F	P	F	P	F
	100	P	F	P	F	P	F	P	F
	0	F	F	F	F	F	F	F	F
	1	P	F	P	F	P	F	P	F
	10	P	F	P	F	P	F	P	F
	100	P	F	P	F	P	F	P	F
		No	Yes	No	Yes	No	Yes	No	Yes
1% Rain water leakage (behind the exterior render)									
letter legend		P :	Pass						
		F :	Fail						
background		short building rain exposure							
color legend		upper part of tall building rain exposure							

Figure 14: Moisture performance and mould growth risk (multi-variable design-assessment chart)

## Conclusion

In this study, the impact of the retrofitting intervention through adding super-insulation panels based on ambient pressure dried aerogels as interior insulation to exterior brick walls on their hygrothermal performance is investigated.

Hereby different wall constructions, different exterior renders, and different climatic and design conditions are varied. The performance of the aerogel-based insulation panel is compared to traditional insulating materials. In the scope of this work single variable parametric studies show that the results are sensitive to the specific simulation case. For that reason a simulation-based multi-variable design assessment chart for mould growth risk is presented.

## Acknowledgement

The research leading to these results has been performed within the HOMESKIN project (<http://homeskin.net/>) and received funding from the European Community's Horizon 2020 Programme (H2020/2014-2020) under grant agreement n° 636709.

## References

- ANSI/ASHRAE Standard 160-2009 Criteria for Moisture-Control Design Analysis in Buildings.
- DIN EN 15026 (2007). Hygrothermal Performance of Building Components and Building Elements—Assessment of Moisture Transfer by Numerical Simulation.
- EN 1609 (2013): Thermal insulating products for building applications - Determination of short term water absorption by partial immersion.
- EN 12086 (2013): Thermal insulating products for building applications - Determination of water vapour transmission properties.
- EN 12087 (2013): Thermal insulating products for building applications - Determination of long term water absorption by immersion. flow meter methods - Products of high and medium thermal resistance.
- EN 12667 (2001): Thermal performance of building materials and products - Determination of thermal resistance by means of guarded hot plate and heat
- EN 13162 (2015): Thermal insulation products for buildings - Factory made mineral wool (MW) products – Specification.
- EN ISO 12572 (2015): Hygrothermal performance of building materials and products - Determination of water vapour transmission properties.
- Galliano, R., Wakili, K. G., Stahl, T., Binder, B., & Daniotti, B. (2016). Performance evaluation of aerogel-based and perlite-based prototyped insulations for internal thermal retrofitting: HMT model validation by monitoring at demo scale. *Energy and Buildings*, 126, 275-286.
- Harrestrup, M. and Svendsen, S. (2016). Internal insulation applied in heritage multi-storey buildings with wooden beams embedded in solid masonry brick façades. *Building and Environment*, 99, 59-72.
- IBP, WUFI® Pro version 5.3, Fraunhofer Institute for Building Physics, Holzkirchen, Germany.
- Ibrahim, M., Biwole, P. H., Achard, P., & Wurtz, E. (2015). Aerogel-based materials for improving the building envelope's thermal behavior: a brief review with a focus on a new aerogel-based rendering. In *Energy Sustainability Through Green Energy* (pp. 163-188). Springer India.
- Johansson, P., Geving, S., Hagetoft, C. E., Jelle, B. P., Rognvik, E., Kalagasidis, A. S., & Time, B. (2014). Interior insulation retrofit of a historical brick wall using vacuum insulation panels: Hygrothermal numerical simulations and laboratory investigations. *Building and Environment*, 79, 31-45.
- Mujeebu, M. A., Ashraf, N., & Alsawayigh, A. (2016). Energy performance and economic viability of nano aerogel glazing and nano vacuum insulation panel in multi-story office building. *Energy*, 113, 949-956.
- NF EN 998-1 (2010). Specification for mortar for masonry. Rendering and plastering mortar.
- Ojanen T, Peuhkuri R, Viitanen H, Lähdesmäki K, Vinha J, Salminen K (2011). Classification of material sensitivity e new approach for mould growth modeling. In: 9th Nordic symposium on building physics, vol. 2, 867-874.
- Toman, J., Vimmrova, A., & Černý, R. (2009). Long-term on-site assessment of hygrothermal performance of interior thermal insulation system without water vapour barrier. *Energy and Buildings*, 41(1), 51-55.
- Van Den Bossche, N., Lacasse, M., Janssens, A. (2011): Watertightness of Masonry Walls: An Overview. *Proceedings 12dbmc Porto*, 8 pp.
- Vereecken E. and Roels S. (2012). Review of mould prediction models and their influence on mould risk evaluation. *Building and Environment* 51, 296-310.
- Vereecken E. and Roels S. (2014), A comparison of the hygric performance of interior insulation systems: a hot box-cold box experiment, *Energy and Buildings* 80, 37-44.
- Viitanen, H. (1996). Factors affecting the development of mould and brown decay in wooden material and wooden structures, Effect of humidity, temperature and exposure time. Doctoral dissertation, Ph. D. thesis. Uppsala, The Swedish University of Agricultural Sciences, Department of Forest Products.
- Viitanen, H., Ojanen, T., Peuhkuri, R., Vinha, J., Lähdesmäki, K., & Salminen, K. (2011). Mould growth modelling to evaluate durability of materials. In *12th International Conference on DBMC. Conference Proceedings* (Vol. 1, pp. 409-416).